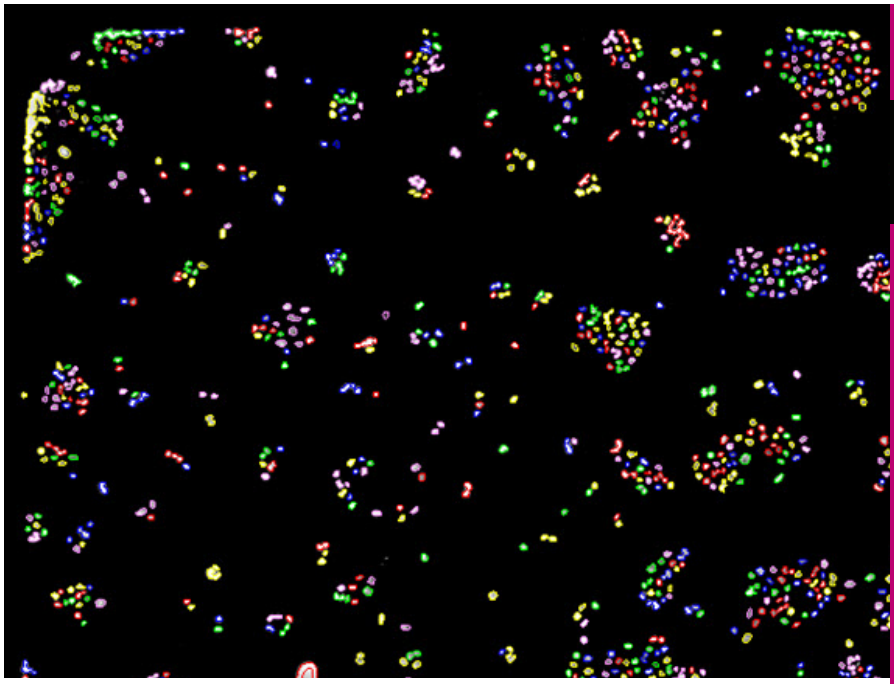

APPLICATION NOTE

Multimode Detection

Authors:

Frauke Haenel

Norbert Garbow

PerkinElmer, Inc.
Hamburg, Germany

Cell Counting and Confluency Analysis as Quality Controls in Cell-Based Assays

Introduction

Multi-parametric cytometrical analysis, such as the determination of cell number or confluency levels, are important quality control parameters in cell-based assays. In order to verify optimal cell handling, confirm cell layer integrity and/or determine the health of cells, image-based analysis should be included in cell-based assay workflows. Cell counting also offers the added benefit of being able to normalize your data to the number of cells in the actual well being measured, leading to less data variability and increased data integrity. The EnSight™ Multimode Plate Reader with well-imaging technology is an ideal instrument for determining important cytometric parameters, such as cell number and confluency level, with or without the use of fluorescent dyes which can sometimes be expensive or toxic.

The EnSight™ system is a versatile benchtop platform that provides a unique combination of well-imaging technology alongside conventional labeled and label-free (cell-based and biochemical) technology. This allows researchers to perform a wide array of target-based and phenotypic assays on one instrument and take a truly orthogonal approach to their research. The well-imaging module provides image-based cytometry capabilities and includes brightfield, digital phase and up to 4 color fluorescent imaging. This enables the determination of inter-well and intra-well cell distribution, investigation of changes in cell morphology, and detection of fluorescent dyes, reporter genes or cell markers. The simple stainless brightfield and digital phase imaging modes permit non-hazardous examination of cell layers at each integral step of the assay workflow. This uncomplicated and seamless system allows the generation of more reliable cell-based assay data for many types of applications. The EnSight system also features Kaleido™ Data Acquisition and Analysis Software, which provides online cellular image evaluation and additionally serves as an instrument control.

PerkinElmer®
For the Better

In this application note, we show how important cytometric parameters, including the determination of cell number and confluency levels per well, can be determined using the EnSight system's brightfield, digital phase and fluorescent imaging modes. More importantly, we provide details on the data acquisition and image evaluation, showing the correlation between different imaging modes and how these approaches uniquely enable the quality control of cell-based assays.

Materials and Methods

Cell Seeding

Cells were either grown in cell culture flasks or seeded into imaging plates from frozen stocks. Cultured cells were grown until they reached sub-confluence, followed by detachment with trypsin. Frozen cells were carefully thawed in a water bath for one min at 37 °C, washed once and re-suspended in cell culture medium containing fetal calf serum (FCS) following regular cell culture protocols. All cell lines were counted with a CASY® Cell Counter (Roche) and were seeded in 30 µl cell culture medium per well in a CellCarrier-384 microplate (PerkinElmer, #6007558). For cell density determination experiments, 2-fold serial dilutions of HeLa and A431 cells were prepared, starting at 40 K cells per well down to 156 cells per well. The plates were incubated under the hood for 20-30 min to allow the cells to settle before the cell number, morphology and distribution was checked in random wells under a standard cell culture microscope. The cells were incubated at 37 °C and 5 % CO_2 for 18-24 hr before fixation and staining.

Fixation

The supernatant on the cells was removed carefully. Cells were then washed once in phosphate buffered saline (PBS) (Sigma-Aldrich, #D8662) and 35 µl of a 4 % formaldehyde (Sigma-Aldrich, #252549) solution in PBS was added to each well. Following a 15-20 min incubation at room temperature, the fixation solution was removed carefully with an electronic multichannel pipette and the cells were washed twice with PBS. Lastly, PBS was added to a final volume of 20 µl per well.

Cell Staining

20 µl of a 4 µg/ml Hoechst 33342 (Life Technologies, #H3570) staining solution in PBS was added to each well (containing 20 µl PBS) and incubated for 20-30 min at 37 °C. Each well was then washed twice in PBS to remove excess stain before plates were sealed and imaged.

Imaging and Instrument Settings

Images were acquired using the EnSight Multimode Plate Reader, equipped with well-imaging module, and Kaleido Data Acquisition and Analysis Software. Details of the Kaleido software settings for each excitation channel used are shown in Table 1.

Table 1. Kaleido software settings for image acquisition of HeLa and A431 cells in a CellCarrier-384 microplate using the brightfield and fluorescence (UV) imaging modes.

Channel	Stain	Light Source
1	None	Brightfield*
2	Hoechst 33342	UV

**The brightfield channel was also used to achieve digital phase images.*

Image Evaluation

The image evaluation algorithms of Kaleido software are based on our Acapella® High Content Imaging and Analysis Software, developed for analysis of high content screening data. Here, we determined the cell number and confluency levels of HeLa and A431 cells based on beta-versions of the image evaluation algorithms shown in Table 2. Secondary data analysis was performed using TIBCO Spotfire® software.

Table 2. Description of Kaleido software image evaluation algorithms used for determination of cell number and confluency.

Evaluation Method	Image Source	Algorithm Details
Count Nuclei	Fluorescent imaging (UV)	Finds stained nuclei and characterizes their number, size and brightness
Determine Confluency	Brightfield imaging	Determines the area covered by cells and provides additional morphology-related information
Count Cells	Digital phase imaging (derived from brightfield imaging)	Localizes cells and provides number and typical size

Results

Whole Well Imaging

Cell number normalization and quality control of cell-based assays require the determination of intra-well and inter-well distribution of cells on a microplate surface. Acquiring one image per well is a fast and sufficient method to capture all cells contained in a well.

The EnSight system is designed to capture almost the entire well of a 96-well plate. With 384-well microplates, the entire well can be captured in one single image, while also providing a convenient magnification to study and monitor cell behavior. Figure 1 shows a raw brightfield image of HeLa cells in a CellCarrier-384 microplate, acquired using the EnSight system. The cell morphology can be easily identified as shown in the enlargement of the original image.

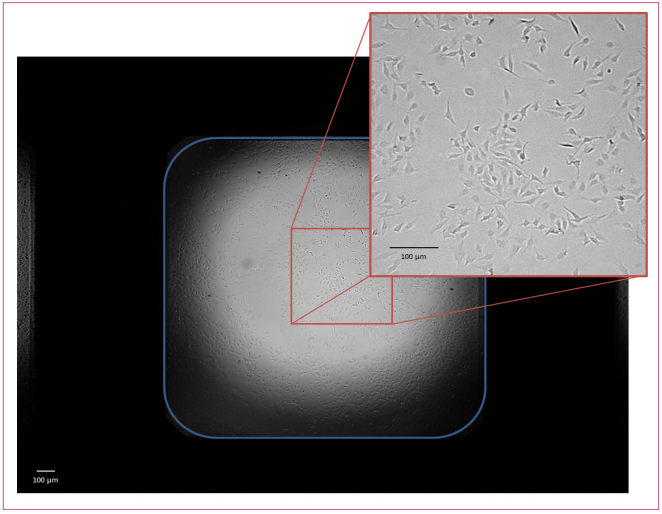

Figure 1. Field of view based on a brightfield image of HeLa cells on a CellCarrier-384 microplate, acquired using the EnSight Multimode Plate Reader with well-imaging technology. The border of the well is indicated in blue. The intensity gradient in the well is caused by the strong curvature of the liquid surface.

Determination of Cell Number and Confluency Level

We have used the EnSight system's three imaging modes; brightfield, digital phase and fluorescent imaging, to investigate cell density characteristics of A431 and HeLa cells in a CellCarrier-384 microplate. Typically, HeLa cells show an even distribution during growth and are considered very suitable for imaging applications. In contrast, A431 cells grow in clusters on uncoated plates making it often difficult to distinguish between individual cells. In the following sections, we show how the cell number and confluency levels of these two distinctly different cell lines were determined.

Cell Counting Utilizing Nucleic Acid Stains

Cell counting on the EnSight system is based on the detection of single nuclei or whole cells. The cell counting algorithms detect either stained nuclei or the whole cells in images that provide phase-contrast characteristics. Nuclei are commonly stained with a dye that binds to nucleic acids. Here, we used Hoechst 33342 (Figure 2).

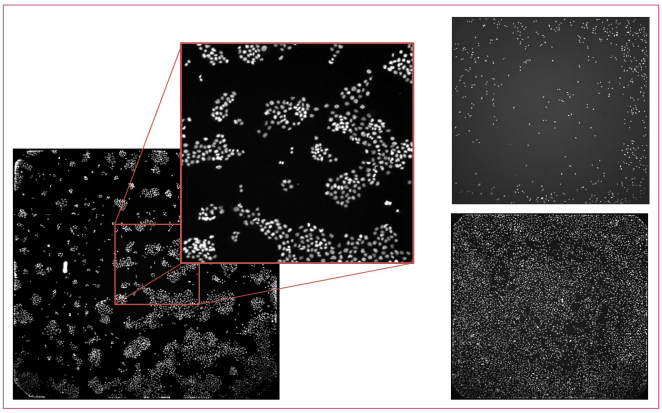

Figure 2. Whole well images of Hoechst 33342-stained A431 and HeLa cells. Left: Hoechst-stained A431 cells (10 K cells per well). Right: Hoechst-stained HeLa cells (Upper panel - 300 cells per well, Lower panel – 10 K cells per well).

The acquired images were then analyzed and single nuclei detected using the *Count Nuclei* algorithm (shown as colored circles in Figure 3). In total, 6439 nuclei were identified for A431 cells and 9326 nuclei for HeLa cells, with 10 K cells per well for each cell line.

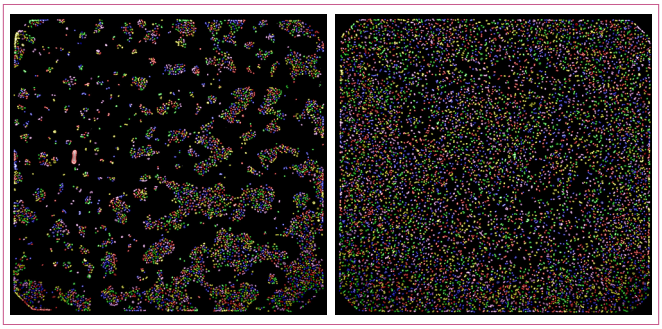

Figure 3. Image segmentation to identify single nuclei, based on the nucleic acid stain Hoechst 33342. Left: Clustered A431 cells (10 K cells per well). Right: homogeneously distributed HeLa cells (10 K cells per well).

Confluency Determination Using Brightfield Imaging

In addition to the cell count based on nucleic acid stains, we also determined the cell confluency in each well, with titrated cells, in brightfield imaging mode. The degree of confluency is defined as the percentage of the image area covered by cells. This mode does not require any stain for the nuclei or cytoplasm of cells and can therefore offer a cost and time saving advantage. It also avoids the toxicity associated with the use of fluorescent stains over long incubation periods.

Figure 4 shows the resulting segmentation of brightfield images of A431 and HeLa cells, following analysis using the *Determine Confluency* algorithm. Both panels in Figure 4 are detailed views of the same wells as shown in Figure 3 (containing 10 K cells per well). The image segmentation determined a confluency of 28.3 % and 77.2 % for A431 and HeLa cells, respectively.

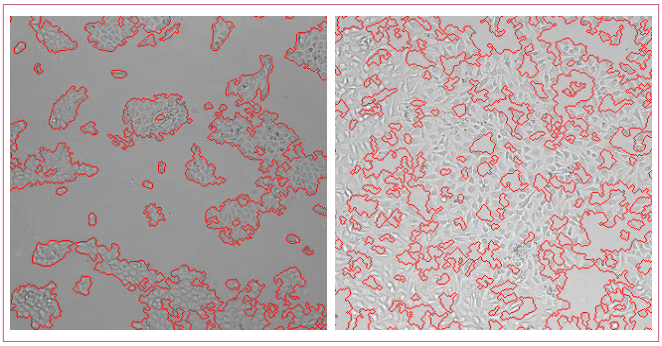

Figure 4. Detailed brightfield images of A431 (left) and HeLa cells (right). The red border illustrates the separation between background and areas covered by cells.

Cell Number Determination Using Digital Phase Imaging

Digital phase data on the EnSight system is calculated based on brightfield images and therefore also does not require any stain. In the resulting images, the cells appear as single objects, which are easy to segment. In Figure 5, the image on the upper left illustrates the results of applying the *Count Cells* algorithm on a calculated digital phase image of A431 cells. Single A431 cells are marked with a colored circle. The image on the upper right shows a calculated digital phase image of HeLa cells without segmentation.

After applying contrast enhancement filters, the resulting digital phase images look similar to images of cells stained with Hoechst 33342 and imaged using fluorescence imaging (Figure 5, lower left and right). The digital phase image segmentation characterizes the cytoplasm rather than the cell nucleus, therefore depending on the cell morphology the identified objects tend to be slightly larger. The images shown in Figure 5 are detailed views of the same wells as shown in Figures 3 and 4 (containing 10 K cells per well). The segmentation of the digital phase images detected 3294 objects for A431 cells, and 6362 objects for HeLa cells.

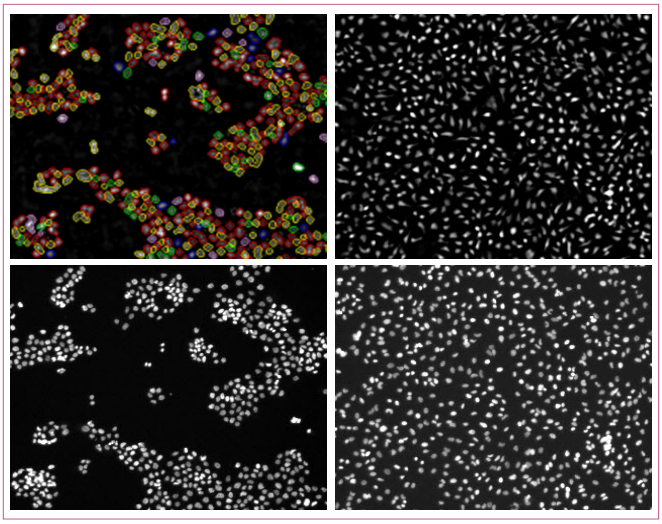

Figure 5. Detailed views of digital phase (top) and fluorescent (bottom) images of A431 (left) and HeLa cells (right). The digital phase and fluorescence (nuclear stain) images are shown for the same region in the wells for both cell lines. For A431 cells, the cell segmentation, based on applying the *Count Cells* algorithm to the digital phase image, is indicated by colored circles (upper left).

Comparison of Cell Density Determination Methods

To understand how the different image evaluation strategies; Nuclei Counting, Confluency Determination and Cell Counting, correlate with each other and with the seeding density, we determined the correlation coefficients (r^2) using TIBCO Spotfire® software. Figure 6 illustrates an example of the correlation between seeding densities of both A431 and HeLa cells and the number of detected objects in digital phase imaging mode. We observed a good correlation, with correlation coefficients of 0.95 for both cell lines tested. The coefficients for the correlation between seeding densities and the different image evaluation methods (using different imaging modes), and for the correlation between different image evaluation strategies, are summarized in Table 3.

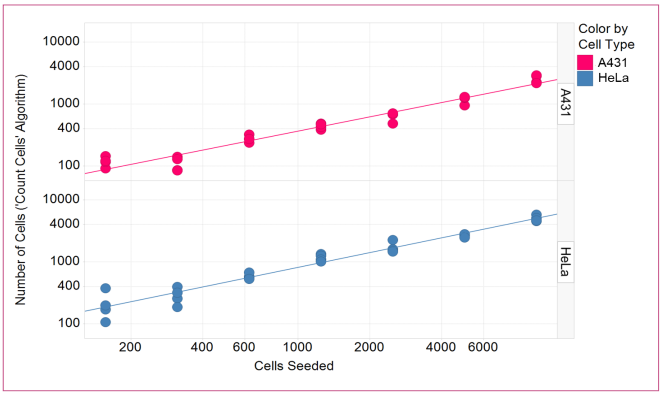

Figure 6. Correlation between seeding density and the number of cells detected in digital phase imaging mode for both A431 (pink) and HeLa cells (blue). Correlation coefficients of 0.95 were determined for both cell lines. With A431 cells in this case, systematically too low cell numbers were found, indicating a non-ideal calibration of the cell counter used in sample preparation.

Table 3. Correlation coefficients were determined to compare the three different image evaluation strategies and the cell seeding densities. Coefficient values are shown in pink for A431 cells and blue for HeLa cells.

Correlation Coefficients	Seeded Cells	Nuclei Count (Flourescent Imaging)	Confluency (Brightfield Imaging)
Nuclei Count (Fluorescent Imaging)	0.96 0.94		
Confluency (Brightfield Imaging)	0.91 0.82	0.91 0.86	
Cell Count (Digital Phase Imaging)	0.95 0.95	0.95 0.97	0.93 0.87

Cell Density Determination As A Quality Control for Cell-Based Assays

The determination of cell seeding density using the EnSight system and the image evaluation methods shown above is a quick and simple tool to ensure assay quality at all steps in your cell-based assay workflow. To illustrate how this tool can be practically applied on a day-to-day basis, and can enable assay control in different situations, we replicated common cell mishandling errors.

Cell Seeding Errors

Cell seeding is a critical step in every cell-based assay, because only equally distributed cells ensure robust assay formats and reliable data. Figure 7 shows how confluency determination using brightfield imaging can be applied to distinguish between wells with correctly seeded cells and wells with incorrect cell seeding numbers. In the center image, an air bubble was trapped in the well during cell seeding, preventing cells from adhering to the well bottom. The bubble disappeared during overnight incubation therefore is not apparent in the image. In the image on the right, the pipette tip scratched the bottom of the plate. In both examples, the mishandling errors lead to a decrease in confluency compared to the control well (Figure 7, left image), as calculated using the image evaluation algorithms described previously.

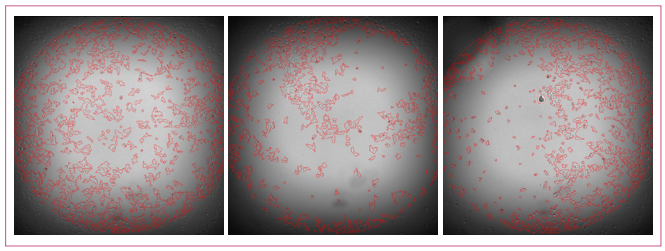

Figure 7. Brightfield images of HeLa cells (1500 cells per well), that were seeded 48 hr before. Correct cell handling (left) results in a confluency of 31.8 %, whereas incorrect cell seeding (center, confluency: 20.5 %) and improper liquid handling (right, confluency: 25.2 %) lead to a decrease in cell confluency.

Bacterial Contamination and Aggregation

Bacterial contamination can also be a common problem when handling cells. Usually, not all wells of a plate are affected by this issue, making it difficult to detect. Determining the confluency of the entire plate prior to the cell assay prevents misleading results. As shown in Figure 8, wells containing MCF-7 cells contaminated with bacteria exhibit an unexpected increase in confluency of up to 90 % compared with the control wells.

An additional parameter, called the "roughness range over well" can also be extracted during the image evaluation. This compares the maximum and minimum of a specific texture parameter within the wells. In cases of bacterial contamination (Figure 8, right), the "roughness range over well" decreases significantly. A similar result is observed if compounds aggregate, as illustrated in Figure 9. When HeLa cells were treated with 100 µM Staurosporine, the compound showed precipitation by eye during pipetting, whereas FCCP at the same concentration did not. For Staurosporine-treated cells (Figure 9, left) the confluency increased whereas the roughness parameter decreased in comparison to FCCP-treated cells (Figure 9, right).

Combining confluency determination with the evaluation of the roughness parameter can be used as an early detection method for bacterial contamination, compound aggregation, and other artifacts that exhibit similar optical properties.

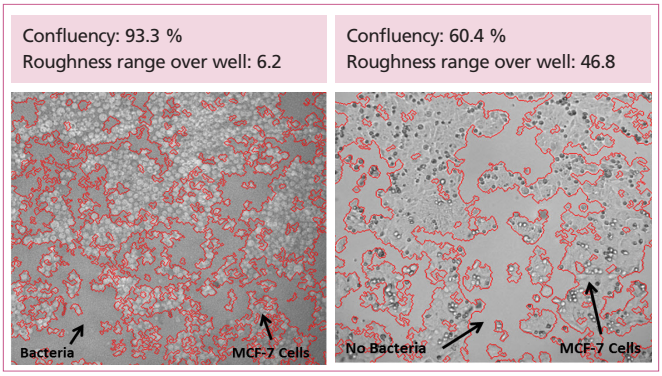

Figure 8. Brightfield images of MCF-7 cells with (left) and without (right) bacterial contamination. The cell confluency segmentation is shown by the red borders. In wells affected by bacterial contamination, the confluency increases, whereas the roughness parameter decreases.

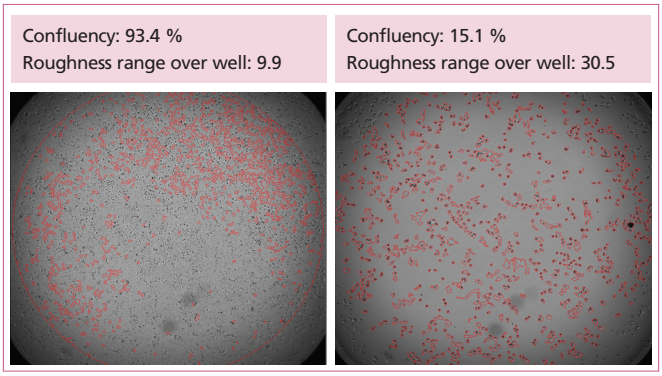

Figure 9. Brightfield images of HeLa cells treated with 100 µM precipitating Staurosporine (left), or 100 µM non-precipitating FCCP (right). Compounds were added in cell culture medium. The cell confluency segmentation is shown by the red borders. If compound precipitation occurs, the confluency increases, whereas the roughness parameter decreases.

Discussion

Here, we demonstrate that cell counting and cell confluency determination using the EnSight Multimode Plate Reader correlate well with seeded cell numbers from 10 K cells per well down to 150 cells per well in a 384-well microplate, using different cell types. Cell numbers greater than 10 K cells per well lead to overconfluent cell layers, making it difficult to identify single objects, and were not included in the correlation results presented here. The difference in absolute cell numbers between seeded and detected A431 cells is based on underestimated cell numbers using the cell counter. This shows how reliably the EnSight system can determine cell numbers, even for cluster-forming cell lines that are difficult to separate.

Using fluorescent imaging of Hoechst 33342-stained nuclei provides robust cell detection in cases where stainless imaging fails, and adds the benefit of allowing analysis of nuclear details and DNA content. In contrast, stainless imaging in the brightfield or digital phase imaging modes has the advantage of being non-toxic, and repetitive or long-term measurements can be applied. Non-toxic determination of cell density is an important parameter during the assay development process, since cell handling often needs to be optimized at several steps of the assay workflow.

We have demonstrated that imperfect cell seeding and liquid handling can be detected by applying cell number and confluency determination using the different imaging modes on the EnSight system. Furthermore, bacterial contamination or aggregating compounds can also be detected reliably by the image evaluation algorithm *Determine Confluency*. With a reading time of only ~4 minutes for an entire 384-well plate, the EnSight system can provide fast and quantitative control data for cell layer integrity with diverse growth morphologies (single cells versus cell clusters). We have shown that the EnSight system enables robust and reliable image evaluation for fluorescent, brightfield and digital phase imaging. With the image-based cytometry capabilities, you can capture the entire well of a 384-well microplate in one image. This ensures fast cell counting or confluency determination independently, on heterogeneous cell distributions within the well.

The evaluation of cell number or confluency can be applied at all steps of your cell-based assay workflow. Combining this parameter with other measurements, such as phenotypic label-free cell-based assays, can provide added confidence and can generate more predictive results by verifying cell viability and cell attachment, or by normalizing assay data to the number of cells detected. Using target-based, orthogonal assay approaches like fluorescence, Alpha technology or time-resolved fluorescence (TRF) in conjunction with imaging enables you to investigate your cell system from many different angles, while also unmasking disruptive artifacts produced by chemical interference. This allows you to make new discoveries faster and easier.

PerkinElmer, Inc.
940 Winter Street
Waltham, MA 02451 USA
P: (800) 762-4000 or
(+1) 203-925-4602
www.perkinelmer.com

PerkinElmer®

For a complete listing of our global offices, visit www.perkinelmer.com/ContactUs

011883_01 September 2014